PAPER

Check for updates

Photochemical reduction of CO_2 into CO coupling with triethanolamine decomposition†

Zhen Li, [ID]* Caili Yang, Yingshi Su, Yonghui Cheng, Yanjia Cui, Suyao Liu and Yiwen Fang

In this work, the impacts of triethanolamine (TEOA) on the performance of photochemical CO_2 reduction were investigated in a simple homogeneous system. We demonstrates that CO_2 can be converted into CO coupling with the decomposition of triethanolamine in TEOA aqueous solution without other additives under light irradiation. About 7.5 μmol CO product is achieved within 7 h with a maximum apparent quantum yield (AQY) of 0.086% at 254 nm. The isotope labelling experiment confirms that CO product originates from the reduction of CO_2 rather than the decomposition of TEOA. In addition, the photochemical system exhibits excellent stability, no obvious inactivation is observed during long-term photochemical CO_2 reduction reaction. This work provides a deep understanding of the effects of TEOA on the performance of photocatalytic CO_2 reduction. Upon utilizing TEOA as a sacrificial electron donor in photocatalytic system, the contribution of TEOA must be considered once evaluating the catalytic activity of catalysts.

Introduction

Artificial photochemical conversion of CO_2 into fuels or value-added chemicals using solar energy is considered as a promising strategy for addressing both energy crisis and environmental issues associated with the consumption of fossil fuels.[1–5] However, the CO_2 reduction reaction faces significant challenges due to the thermodynamic stability and low reactivity of CO_2 molecule. To overcome these challenges, researchers have been focusing on the development of photochemical systems, including homogeneous and heterogeneous systems. The homogeneous system, which involves molecular catalysts, has gained attention due to its advantages in high activity, selectivity, tunable structure, and trackable chemical reactivity.[6,7]

Generally, a typical homogeneous photochemical system for CO_2 reduction includes a photosensitizer, a sacrificial reductant, and a molecular catalyst. Designing effective molecular catalysts has been a key focus in achieving high activity and selectivity for CO_2 reduction. In the past decades, various types of catalysts, such as metal pyridyl complexes,[8,9] metal porphyrin catalysts,[10] metal salen complexes,[11,12] imidazolium salts,[13] and ionic liquids,[14,15] have been developed and shown excellent

catalytic activity in homogeneous systems. In these photochemical systems, molecular complexes usually exhibit dual function. First, molecular catalyst can function as a photosensitizer, which converts solar light into chemical energy for CO_2 reduction. While the metal center of the complex acts as an active site, transferring the photoinduced electron into the reduction reaction of CO_2. In addition, it is crucial to ensure the rapid acceptance of an additional electron from sacrificial electron donors to avoid the accumulation of charge carriers, which can induce catalyst decomposition and diminish the durability of the photocatalytic system.[16,17] TEOA, acting as a sacrificial reductive quencher for chromophore excited states, is commonly used as an electron donor in photochemical CO_2 reduction reaction. However, it should be noted that previous reports have overlooked the potential secondary roles of TEOA in photochemical CO_2 reduction performance. In other words, TEOA might directly reduce CO_2 under light irradiation. Thereby, further research is needed to fully understand the potential applications and contributions of TEOA in photochemical CO_2 reduction mechanisms.

Herein, the effects of TEOA on the performance of homogeneous photochemical CO_2 reduction were studied in detail. The gaseous and liquid products were analyzed by ^{1}H and ^{13}C nuclear magnetic resonance (NMR) spectroscopy, mass spectroscopy (MS), attenuated total reflectance Fourier transform infrared spectroscopy (ATR-FTIR), and gas chromatography (GC). These studies collectively provide a comprehensive understanding of the reaction mechanism during the photochemical CO_2 reduction in the presence of TEOA aqueous solution without other additives.

Department of Chemistry and Key Laboratory for Preparation and Application of Ordered Structural Materials of Guangdong Province, Shantou University, Shantou 515063, China. E-mail: lizhenlicp@stu.edu.cn
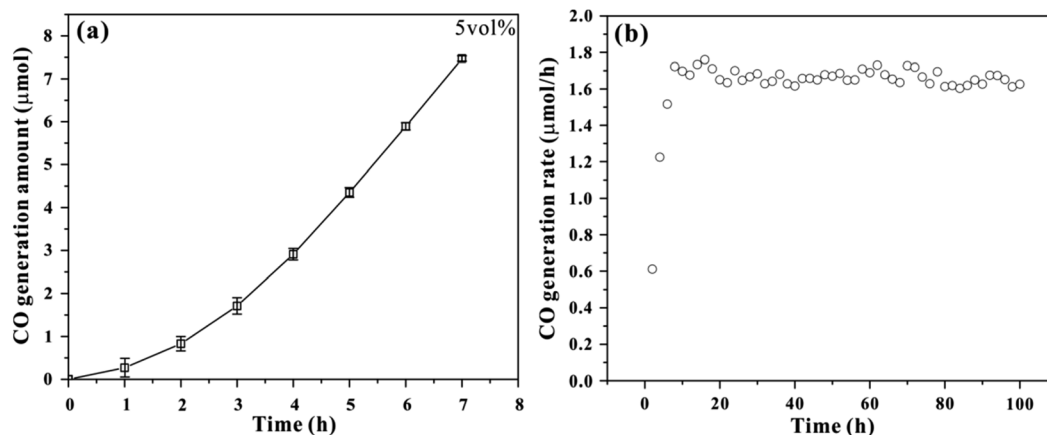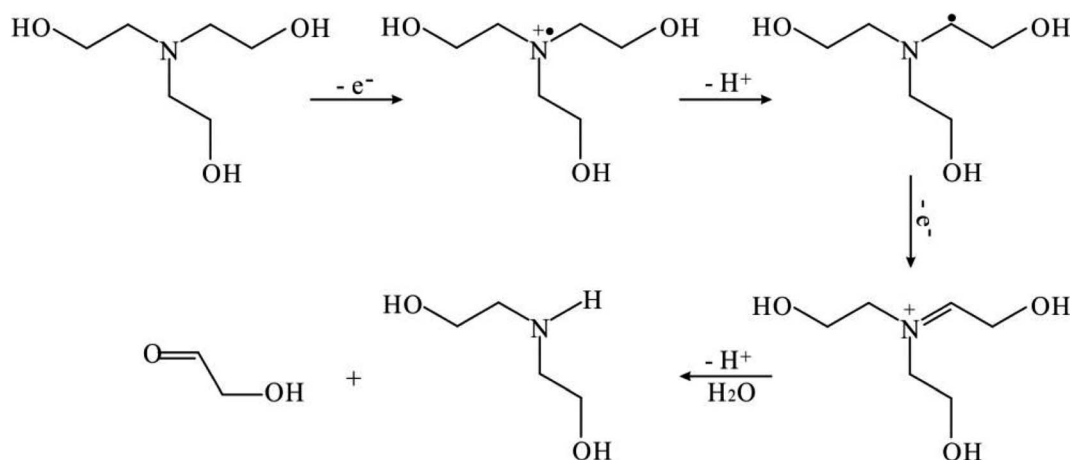
Fig. 1 (a) Time-dependent performance of photochemical CO_2 reduction in 5 vol% TEOA aqueous solution under light irradiation. The error bars represent the standard deviation of three separate measurements. (b) The stability investigation during photochemical CO_2 reduction in 5 vol% TEOA aqueous solution under light irradiation.

Scheme 1 The decomposition pathway of TEOA upon monoelectronic oxidation.

Results and discussion

We first optimized the performance of photochemical CO_2 reduction in a 250 mL custom-built cell with different volume ratio of TEOA and H_2O (Fig. S1–S3†). A 300 W Xe lamp was used as the irradiation source, and the irradiation area was 12.5 cm^2. It can be observed that the generation rate of CO exhibits similar trend in three photochemical systems, which increases upon increasing irradiation time. About 1.29, 1.58 and 1.65 μmol h^{-1} of CO generation rates are achieved at 7 h irradiation, corresponding to 3, 5 and 10 vol% TEOA aqueous solution respectively. As a result, 5 vol% TEOA aqueous solution system was applied for the following comparison. The UV-vis absorption spectrum was performed to monitor reaction intermediate. As depicted in Fig. S4,† the original TEOA aqueous solution mainly absorb ultraviolet light below 275 nm. Upon irradiation, a new absorption band emerges, possibly attributed to the formation of carbamate species.[18,19] The peak intensity gradually increases with prolonged irradiation time and reaches a maximum at 7 h irradiation. Such evolution is consistent with

that of CO_2 generation rate, suggesting the presence of carbamate intermediate.

Fig. 1a shows the time-dependent CO generation amount during photochemical CO_2 reduction reaction in 5 vol% TEOA aqueous solution under light irradiation. About 7.5 μmol CO product is achieved within the testing time frame. Note that the initial rate for CO generation is low at the first 3 h of photochemical reaction, which may be associated to an induced period.[20] The quasi-linear plot of CO generation amount with irradiation time implies CO gas comes from photochemical reduction.[21] Table S1† summarizes the photochemical CO_2 reduction under different sets of conditions. The result suggests that the TEOA aqueous solution systems exhibit significant performance in the conversion of CO_2 into CO under light irradiation. However, no CO product is detected (entry 4) after equipping with a cut-off filter ($\lambda > 420$ nm), implying that this photochemical reaction needs to be initiated by ultraviolet light, which is supported by the test of UV-vis absorption spectrum. Once CO_2 is replaced with N_2 (entry 5), no detectable CO is observed, suggesting that CO_2 serves as the carbon source in our

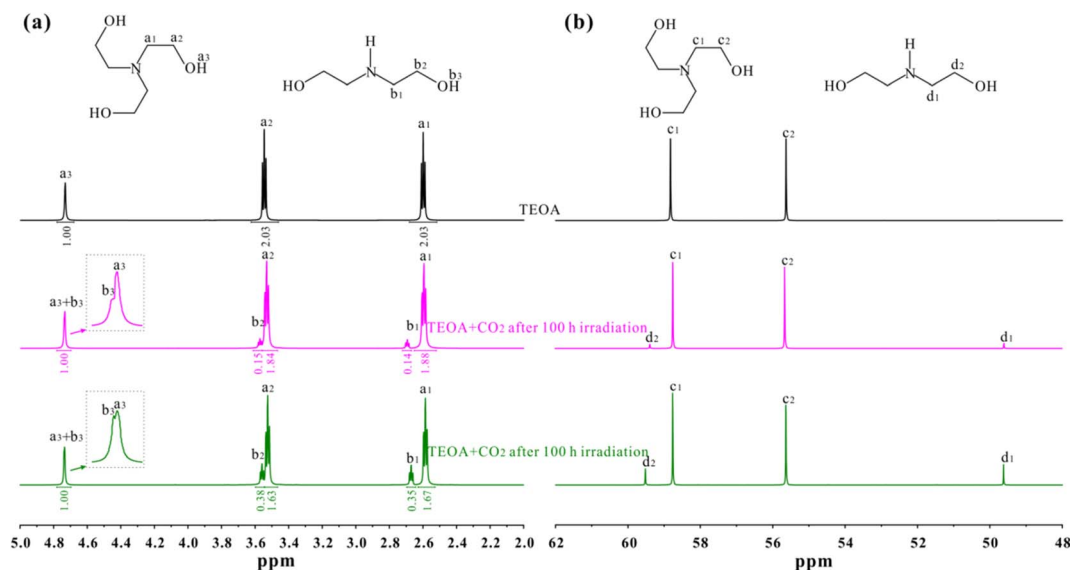**Fig. 2** (a) ^{1}H and (b) ^{13}C NMR spectra of pure TEOA, TEOA after 12 or 100 h irradiation under CO_2 bubbling condition. The solution consists of 100 μL TEOA and 500 μL D_2O. The TEOA after photochemical reaction in 5 vol% TEOA aqueous solution is achieved by freeze-drying for 48 h to remove residual water.

photochemical reaction, in other words, the CO product originates from CO_2 rather than the decomposition of TEOA. In order to confirm that CO is generated exclusively from CO_2, the isotope labeling experiment of $^{13}CO_2$ gas was conducted as shown in Fig. S5.† The mass spectra presents one peak at $m/z = 29$ assigned to ^{13}CO, verifying that the CO product comes from the reduction of CO_2 molecule. The apparent quantum yield (AQY) was performed with a 300 W Xe lamp irradiation equipped with various band-pass filters (254, 275, 295, 313, 350, 365 and 380 nm) as depicted in Table S2.† The result suggests that this photochemical system exhibits low AQY value, and the maximum AQY of CO generation is calculated to be 0.086% at 254 nm. In addition, the stability of the photochemical system was performed as shown in Fig. 1b, there is no obvious inactivation during photochemical CO_2 reduction process after 100 h irradiation, suggesting the robustness of this photochemical system.

Note that the sources of protons and electrons are required during CO_2 reduction reaction because they play a vital role in enabling the deoxygenation process of CO_2 molecule. The primary source of the protons can be attributed to H_2O or TEOA in our photochemical system. However, the electron can only come from TEOA molecule rather than H_2O since no oxygen has been detected during CO generation. In particular, TEOA can donate two protons and two electrons during its decomposition (see Scheme 1).[22–25] Therefore, we speculate that the electrons from TEOA decomposition participate in CO_2 reduction reaction.

In order to confirm this point, ^{1}H and ^{13}C NMR spectra of pure TEOA, TEOA after 12 h irradiation and TEOA after 100 h irradiation were recorded on a Bruker 600 MHz spectrometer as shown in Fig. 2. Prior to test, the solution after irradiation was freeze-dried for 48 h to remove residual water. In Fig. 2a, three ^{1}H NMR signals are observed for pure TEOA, the peaks centred

at 4.73, 3.55 and 2.60 ppm are attributed to OH, O–CH_2 and N–CH_2 groups according to previous reports.[26–29] After 12 h irradiation under CO_2 bubbling condition, two new signals are monitored, one peak at 3.58 ppm is assigned to O–CH_2 group, while the other at 2.68 ppm is assigned to N–CH_2 groups in diethanolamine (DEOA) molecules. However, the OH signal of DEOA disappears due to its overlaps with TEOA, as supported by the area integration analysis and the inserted figure in Fig. 2a. After 100 h irradiation under CO_2 bubbling condition, the peak intensity of DEOA is significantly enhanced. The results indicate the presence of DEOA in the solution after irradiation. Furthermore, the content of DEOA increases once prolonging the irradiation time. This observation suggests that the photochemical CO_2 reduction reaction leads to the decomposition of TEOA. It is also confirmed by ^{13}C NMR spectra shown in Fig. 2b, two ^{13}C NMR signals are detected for pure TEOA, the peaks centred at 58.82 and 55.62 ppm are attributed to N–CH_2 and O–CH_2 groups of TEOA molecules, respectively.[30–32] After 12 h irradiation under CO_2 bubbling condition, two new signals are observed, one peak at 59.49 ppm is assigned to O–CH_2 group, while the other at 49.62 ppm is assigned to N–CH_2 groups in DEOA molecules. Similarly, the peak intensity of DEOA is significantly enhanced after 100 h irradiation under CO_2 bubbling condition.

The ATR-FTIR spectra were also performed to study the decomposition of TEOA as shown in Fig. S6.† For pure TEOA, it shows the typical vibration modes of TEOA molecules, consistent with previous reports.[33] After 12 h irradiation under CO_2 bubbling condition, two new peaks centred at 1647 and 1544 cm^{-1} are observed, which derives from the vibration modes of N–H deformation in DEOA molecules and C=O stretching in $NCOO^-$ group[34–36] that generated from the adsorption of CO_2 by amine species.[29] While their intensity
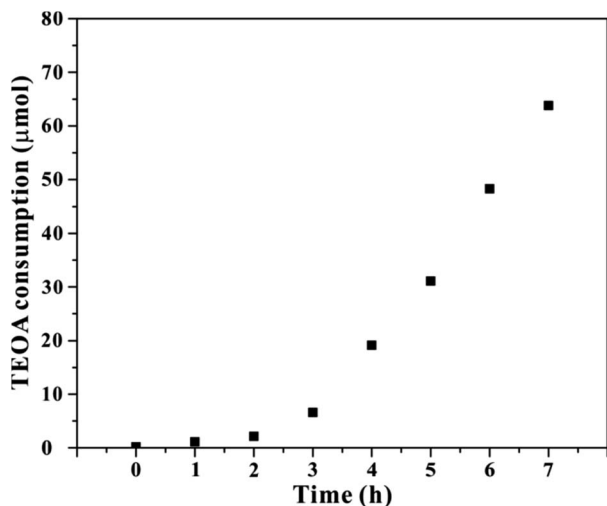
Fig. 3 The time-depended consumption during photochemical CO_2 reduction in 5 vol% TEOA aqueous solution under light irradiation.

increases as irradiation proceeds, proving that the formation process of DEOA is caused by photochemical reaction. In addition, the ESI-MS spectra were applied to further confirm the formation of DEOA from the decomposition of TEOA as shown in Fig. S7–S9.† For pure TEOA, the signals at $m/z = 150$ and 172 correspond to TEOA, while the new signal at $m/z = 106$ was attributed to DEOA after light irradiation.

To identify the photochemical process is stoichiometric in TEOA aqueous solution, the amount of TEOA was monitored during photochemical CO_2 reduction by ^1H NMR technique. As a result, the standard curves for different amount of TEOA was quantified by the peak area as shown in Fig. S10.† Fig. 3 presented the decomposition amount of TEOA, which is determined by subtracting the remaining TEOA quantity from the initial total TEOA content within the system. As we can see, about 63.7 μmol TEOA is consumed within the testing time frame. This value is much higher than that of CO generation amount as shown in Fig. 1, suggesting the photochemical CO_2 reduction reaction is nonstoichiometric in TEOA aqueous solution. This is possibly caused by the self-decomposition of excited TEOA molecules.[37–39] Nonetheless, it exhibited similar trend with the CO generation amount, implying the photochemical reduction of CO_2 into CO coupled with TEOA decomposition.

According to the previous reports[40–43] and our experimental results, a possible mechanism for photochemical CO_2 reduction in our system is proposed in Scheme 2. TEOA firstly adsorbs CO_2 molecules to form carbamate, which subsequently converts into a positively charged aminyl radical (TEOA$^{•+}$) and carbon dioxide radical anions ($CO_2^{•-}$) by a monoelectronic transfer under UV light irradiation condition. Then the deprotonation of the TEOA$^{•+}$ transfers into a carbon centered radical via rearrangement,[44] which will contribute to the deoxygenation of $CO_2^{•-}$ to generate CO product. Subsequently, the iminium species further degrades into glycolaldehyde and DEOA in the present of H_2O.
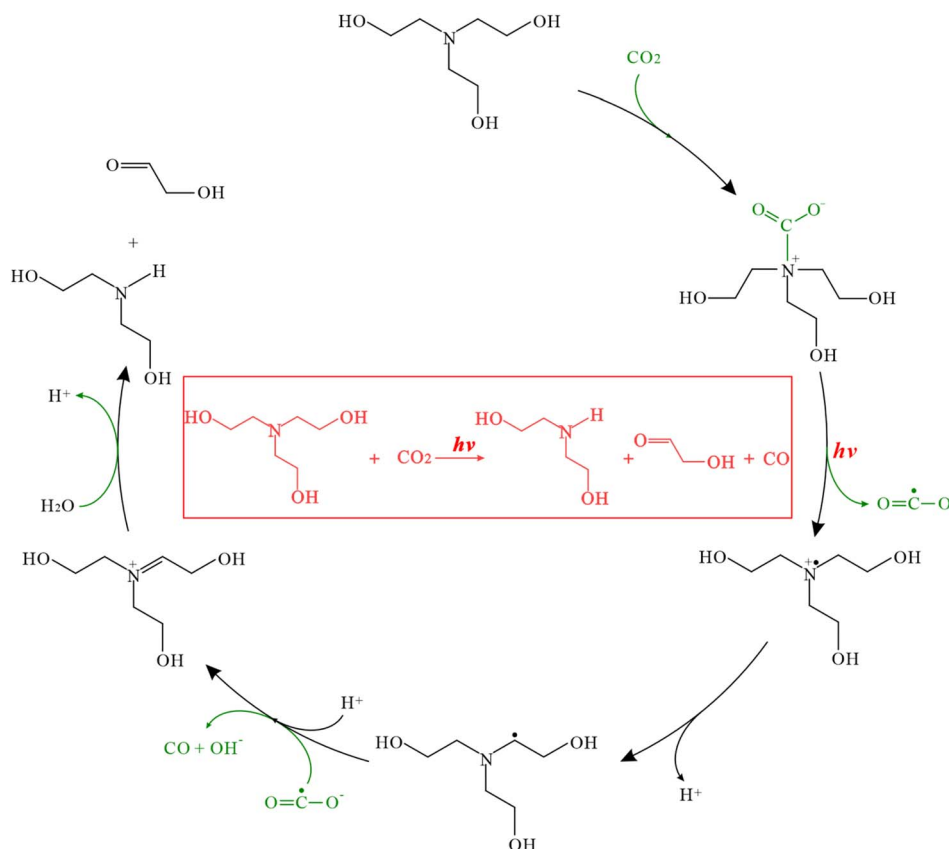
Scheme 2 Proposed mechanism for CO_2 reduction coupling with TEOA decomposition.

Conclusion

In summary, our work demonstrates that CO_2 can be converted into CO in a TEOA aqueous solution under light irradiation without other additives. The isotope labelling experiment confirms the CO product originates from CO_2 rather than the decomposition of TEOA. This photochemical system exhibits excellent stability during long-term photochemical CO_2 reduction reaction. In addition, the decomposition of TEOA was also analyzed by ^1H and ^{13}C NMR, MS and ATR-FTIR. At last, a possible mechanism is proposed for CO_2 reduction coupling with TEOA decomposition. We believe that this work will provide a deep understanding of the effects of TEOA on the performance of photocatalytic CO_2 reduction. When TEOA is served as a sacrificial electron donor in photocatalytic system, the investigation of intrinsic activity for catalyst needs to take TEOA contributions into consideration.

Author contributions

C. L. Yang: investigation, validation, data analysis, writing. Y. S. Su, Y. H. Cheng, Y. J. Cui: investigation. S. Y. Liu, Y. W. Fang: supervision. Z. Li: review, editing, supervision, project administration, funding acquisition.

Conflicts of interest

There are no conflicts to declare.

Acknowledgements

References

1 T. Wang, L. Zhang, J. Liu, X. X. Li, L. Yuan, S. L. Li and Y. Q. Lan, *Chem. Commun.*, 2022, **58**, 7507–7510.

2 C. C. Lin, T. R. Liu, S. R. Lin, K. M. Boopathi, C. H. Chiang, W. Y. Tzeng, W. H. C. Chien, H. S. Hsu, C. W. Luo, H. Y. Tsai, H. A. Chen, P. C. Kuo, J. Shiue, J. W. Chiou, W. F. Pong, C. C. Chen and C. W. Chen, *J. Am. Chem. Soc.*, 2022, **144**, 15718–15726.

3 Q. Y. Ge, Y. Y. Liu, K. J. Li, L. F. Xie, X. J. Ruan, W. Wang, L. Q. Wang, T. Wang, W. B. You and L. W. Zhang, *Angew. Chem., Int. Ed.*, 2023, **62**, e202304189.

4 A. Sole-Daura, Y. Benseghir, M. H. Ha-Thi, M. Fontecave, P. Mialane, A. Dolbecq and C. Mellot-Draznieks, *ACS Catal.*, 2022, **12**, 9244–9255.

5 L. K. Putri, B. J. Ng, W. J. Ong, S. P. Chai and A. R. Mohamed, *Adv. Energy Mater.*, 2022, **12**, 2201093.

6 B. Ma, M. Blanco, L. Calvillo, L. J. Chen, G. Chen, T. C. Lau, G. Drazic, J. Bonin, M. Robert and G. Granozzi, *J. Am. Chem. Soc.*, 2021, **143**, 8414–8425.

7 D. J. Cole-Hamilton, *Science*, 2003, **299**, 1702–1706.

8 A. C. Tsipis and A. A. Sarantou, *Dalton Trans.*, 2021, **50**, 14797–14809.

9 N. Elgrishi, M. B. Chambers, X. Wang and M. Fontecave, *Chem. Soc. Rev.*, 2017, **46**, 761–796.

10 C. Maeda, T. Taniguchi, K. Ogawa and T. Ema, *Angew. Chem., Int. Ed.*, 2015, **54**, 134–138.

11 M. North, S. C. Z. Quek, N. E. Pridmore, A. C. Whitwood and X. Wu, *ACS Catal.*, 2015, **5**, 3398–3402.

12 C. J. Whiteoak, N. Kielland, V. Laserna, E. C. Escudero-Adán, E. Martin and A. W. Kleij, *J. Am. Chem. Soc.*, 2013, **135**, 1228–1231.

13 F. D. Bobbink, D. Vasilyev, M. Hulla, S. Chamam, F. Menoud, G. Laurenczy, S. Katsyuba and P. J. Dyson, *ACS Catal.*, 2018, **8**, 2589–2594.

14 M. H. Anthofer, M. E. Wilhelm, M. Cokoja, M. Drees, W. A. Herrmann and F. E. Kühn, *ChemCatChem*, 2015, **7**, 94–98.

15 Z. Z. Yang, Y. F. Zhao, G. P. Ji, H. Y. Zhang, B. Yu, X. Gao and Z. M. Liu, *Green Chem.*, 2014, **16**, 3724–3728.

16 M. Takahashi, T. Asatani, T. Morimoto, Y. Kamakura, K. Fujii, M. Yashima, N. Hosokawa, Y. Tamaki and O. Ishitani, *Chem. Sci.*, 2023, **14**, 691–704.

17 M. Pschenitza, S. Meister and B. Rieger, *Chem. Commun.*, 2018, **54**, 3323–3326.

18 H. J. Kwon, J. R. Cha and M. S. Gong, *Polymer*, 2017, **113**, 4313–4322.

19 K. H. Chae and Y. H. Kim, *Adv. Funct. Mater.*, 2007, **17**, 3470–3476.

20 S. X. Min and G. X. Lu, *J. Phys. Chem. C*, 2011, **115**, 13938–13945.

21 Z. G. Liu, J. Y. Li, Z. Y. Chen, M. Y. Li, L. Z. Wang, S. Q. Wu and J. L. Zhang, *Appl. Catal., B*, 2023, **326**, 122338.

22 P. W. Du, J. Schneider, P. Jarosz and R. Eisenberg, *J. Am. Chem. Soc.*, 2006, **128**, 7726–7727.

23 K. Kalyanasundaram, J. Kiwi and M. Grätzel, *Helv. Chim. Acta*, 1978, **61**, 2727–2730.

24 E. D. Cline, S. E. Adamson and S. Bernhard, *Inorg. Chem.*, 2008, **47**, 10378–10388.

25 D. G. Whitten, *Acc. Chem. Res.*, 1980, **13**, 83–90.

26 Y. S. Ge, G. Cheng and H. Z. Ke, *J. CO2 Util.*, 2022, **57**, 101873.

27 A. García-Abuín, D. Gomez-Díaz, A. B. Lopez, J. M. Navaza and A. Rumbo, *Ind. Eng. Chem. Res.*, 2013, **52**, 13432–13438.

28 C. Chatterjee and A. Sen, *J. Mater. Chem. A*, 2015, **3**, 5642–5647.

29 J. H. Choi, S. G. Oh, Y. E. Kim, Y. I. Yoon and S. C. Nam, *Environ. Eng. Sci.*, 2012, **29**, 328–334.

30 A. U. Maheswari and K. Palanivelu, *J. CO2 Util.*, 2014, **6**, 45–52.

31 G. Szalontai, G. Kiss and L. Bartha, *Spectrochim. Acta, Part A*, 2003, **59**, 1995–2007.

32 P. V. Kortunov, L. S. Baugh, M. Siskin and D. C. Calabro, *Energy Fuels*, 2015, **29**, 5967–5989.

33 S. Ahmed, A. Ramli and S. Yusup, *Int. J. Greenhouse Gas Control*, 2016, **51**, 230–238.

34 G. G. Qi, Y. B. Wang, L. Estevez, X. N. Duan, N. Anako, A. H. A. Park, W. Li, C. W. Jones and E. P. Giannelis, *Energy Environ. Sci.*, 2011, **4**, 444–452.

35 A. Zhao, A. Samanta, P. Sarkar and R. Gupta, *Ind. Eng. Chem. Res.*, 2013, **52**, 6480–6491.

36 H. He, C. Liu, M. E. Louis and G. H. Li, *J. Mol. Catal. A: Chem.*, 2014, **395**, 145–150.

37 Q. Y. Li, Z. L. Jin, Z. G. Peng, Y. X. Li, S. B. Li and G. X. Lu, *J. Phys. Chem. C*, 2007, **111**, 8237–8241.

38 X. J. Zhang, Z. L. Jin, Y. X. Li, S. B. Li and G. X. Lu, *J. Phys. Chem. C*, 2009, **113**, 2630–2635.

39 Q. Y. Li, L. Chen and G. X. Lu, *J. Phys. Chem. C*, 2007, **111**, 11494–11499.

40 A. Miyaji and Y. Amao, *New J. Chem.*, 2021, **45**, 5780–5790.

41 Y. Pellegrin and F. Odobel, *C. R. Chim.*, 2017, **20**, 283–295.

42 B. H. Zhao, Y. Huang, D. L. Liu, Y. F. Yu and B. Zhang, *Sci. China: Chem.*, 2020, **63**, 28–34.

43 Y. X. Pan, Y. You, S. Xin, Y. T. Li, G. T. Fu, Z. M. Cui, Y. L. Men, F. F. Cao, S. H. Yu and J. B. Goodenough, *J. Am. Chem. Soc.*, 2017, **139**, 4123–4129.

44 P. J. Delaive, T. K. Foreman, C. Giannotti and D. G. Whitten, *J. Am. Chem. Soc.*, 1980, **102**, 5627–5631.